Modeling the role of mortality-based response triggers on the effectiveness of African swine fever control strategies

Running head: The spread of African swine fever in Brazil

Gustavo Machado[1]*§, Trevor Farthing [1]§, Mathieu Andraud[2], Francisco Paulo Nunes Lopes [3], Cristina Lanzas[1]

[1]North Carolina State University, Department of Population Health and Pathobiology, College of Veterinary Medicine, Raleigh, North Carolina.

[2]Anses, French Agency for Food, Environmental and Occupational Health & Safety, Ploufragan-Plouzané-Niort Laboratory, Epidemiology, Health and Welfare research unit, F22440, Ploufragan, France.

[3] Departamento de Defesa Agropecuária, Secretaria da Agricultura, Pecuária e Desenvolvimento Rural, Porto Alegre, Brazil

Corresponding author: Dr. Gustavo Machado, gmachad@ncsu.edu - § shared first author

African swine fever (ASF) is considered the most impactful transboundary swine disease. In the absence of effective vaccines, control strategies are heavily dependent on mass depopulation and movement restrictions. Here we developed a nested multiscale model for the transmission of ASF, combining spatially explicit network model of animal movements with a deterministic compartmental model for the dynamics of two ASF strains within-pixels of 3 km x 3 km, amongst the pig population in one Brazilian state. The model outcomes are epidemic duration, number of secondary infected farms and pigs, and distance of ASF spread. The model also predicted the spatial distribution of ASF epidemics. We analyzed quarantine-based control interventions in the context of mortality trigger thresholds for the deployment of control strategies.

The mean epidemic duration of a moderately virulent strain was 11.2 days assuming the first infection is detected (best-case scenario) and 15.9 days when detection is triggered at 10 % mortality. For a highly virulent strain, the epidemic duration was 6.5 days and 13.1 days, respectively. The distance from the source to infected locations and the spatial distribution was not

dependent on strain virulence. Under the best-case scenario, we projected an average number of infected farms of 18.79 farms and 23.77 farms for the moderate and highly virulent strains, respectively. At 10% mortality-trigger, the predicted number of infected farms was on average 48.28 farms and 42.97 farms, respectively. We also demonstrated that the establishment of ring quarantine zones regardless of size (i.e., 5 km, 15 km) was outperformed by backward animal movement tracking. The proposed modeling framework provides an evaluation of ASF epidemic potential, providing a ranking of quarantine-based control strategies that could assist animal health authorities in planning the national preparedness and response plan.

Keywords: network modeling, swine disease dynamics, surveillance, secure business continuity.

Introduction

African swine fever (ASF) has not been reported in South America since the 1980s (Costard et al., 2009), but it is widespread in the northern hemisphere, including most of Asia (Mighell and Ward, 2021), and stretched as far as Germany, where it continues to infect wild boars and domestic pigs throughout several countries (Gao et al., 2020; Sauter-Louis et al., 2020). The rapid spread of ASF throughout the northern hemisphere (Yoon et al., 2020) has reignited concerns about ASF reintroduction into the Americas.

The main modes of ASF transmission are direct contact with infected animals, ingestion of infected pork products and or residuals, and contact with contaminated fomites (Chenais et al., 2019). In infected areas, between-farm pig transportation has been described as the major pathway of ASF propagation (Andraud et al., 2019; Chenais et al., 2019; Hayes et al., 2020; Liu et al., 2020). In addition, the swine population in ASF-free regions is immunologically naive as there are no effective vaccines (Dellicour et al., 2020; Dixon et al., 2020). All these factors make controlling the spread of ASF a very challenging problem. In European and North American countries, ASF response plans include national movement standstill, testing, and stamping out, pre-emptive depopulation of neighboring herds, enhanced surveillance in predefined control zones, contact tracing, and the enhancement of on-farm biosecurity (Gallardo et al., 2015; Bellini et al., 2016; Halasa et al., 2016a; Sánchez-Cordón et al., 2018; USDA-APHIS, 2020).

Evaluating the effectiveness and economic impact of control strategies (e.g., animal movement restrictions, mass depopulation) have been among the priorities for ASF-free

countries like the USA and Brazil (Halasa et al., 2018a; Hayes et al., 2020; USDA-APHIS, 2020). In this vein, disease spread simulation models have been widely used to study transmission dynamics and to evaluate control options (Bradhurst et al., 2015; Machado et al., 2020; Galvis, Prada et al., 2021), several examples of model outputs implementation are described (Heesterbeek et al., 2015; Ezanno et al., 2020; Galvis et al., 2020; Halasa, Græsbøll et al., 2020; Hayes et al., 2020). Disease detection based on pig mortality and clinical disease has been recommended as the most effective surveillance option for disease response to trigger subsequent investigations and stamping out of affected herds (Guinat et al., 2017; Nielsen et al., 2017; USDA-APHIS, 2020; European Commission, 2020). The effectiveness of using mortality data for early detection of ASF is supported by additional modeling studies (Guinat et al., 2018; Faverjon et al., 2020).

Even though mathematical models have been proposed to estimate epidemiological consequences of ASF introduction in European countries (Halasa et al., 2016a, 2018a; Andraud et al., 2019), there are gaps in such models mainly because known variations on ASF clinical presentation and mortality patterns were not considered, such differences depend on multiple factors, including route and dose of viral infection, the virulence of the stain, as well as host and population factors (Salguero, 2020; Mighell and Ward, 2021). In this study, we developed a nested multiscale model for the transmission of two ASF strains, with distinct virulence characteristics. Transmission among pixels is represented by a spatially explicit network model of animal movements. The spatial unit was defined as 3 km x 3 km gridded cells (pixel), in which the within-pixel ASF dynamics are represented by a deterministic compartmental model. The model provides epidemic duration, secondary infections, and distance spread across all pig populations of one Brazilian state. We also investigated how early detection based on mortality thresholds affects future epidemic outcomes while producing maps of secondary cases. Finally, we compared and contrasted different control strategies, namely: established control zones, contact tracing, with different surveillance mortality-base trigger thresholds scenarios, and both ASF strains. We demonstrate the utility of spatially explicit models in producing maps to guide preparedness activities in ASF-free regions. All results are presented in the context of mortality-trigger and virulence combinations.

Material and Methods

In the sections below we describe i) data sources used to recreate the temporally-dynamic pig shipment network model; ii) the design and parameterization of the ASF transmission model simulated on the between-farm movement network; iii) the model inputs we used to simulate the spread of ASF strains, and iv) the model output and analyses employed to assess the disease control scenarios.

Study areas and animal movement data

The study area comprises the swine population of Rio Grande do Sul, Brazil, the state holds nearly 15% of the national commercial pig population. More details about the pig population and a detailed description of the multiyear between farm pig movements networks are described elsewhere (Machado et al., 2020). Here, we reconstructed the between-farm pig transportation network describing animal shipments from Jan. 2nd, 2015 until Dec 31st, 2018. This network describes a total of 273,158 shipments between 13,111 registered swine farms. For each individual pig farm, we identified: farm geolocation, for commercial operations pig company name to which the farm(s) are contracted with, pig capacity, and the number of pigs per premise, from the local official veterinary service (SEAPI-RS, 2018). Farms declared inactive, in which no pigs raised in the past two years or out of business, were not considered in the analysis. Movements from or to other states were also excluded, given the lack of information about farm registration outside the Rio Grando do Sul state lines.

The study area, the entire state of Rio Grande do Sul (Figure 1), was divided into gridded 3 km x 3 km cells (pixels) to which the between-farm pig movements were aggregated. Briefly, each farm location was intersected into one of the 4,367 unique 3-km pixels containing at least one pig farm. The 3-km pixel size was based on previous work (Halasa et al., 2016a), in which extensive sensitivity analyses suggested that a distance of up to 2 km around infected farms adequately capture the mixture of unregistered animal movements, shared equipment, and tools, people or sharing of equipment between neighbors, and local transmission events driven by rodents and insects and other wildlife hosts. Thus, by creating a pixel-level network, we were able to minimize computational requirements without sacrificing model realism. The pixel-level network consisted of 259,004 temporally-dynamic daily directed edges between the 4,367 pixels. For modeling purposes, we calculated the maximum pig-holding capacity of all farms within each pixel and appended this information to the networks as a node-level variable to be used as a

proxy for swine population size. For each pixel, we also identified what swine production companies operated ≥ 1 farm contained therein and appended this information to nodes as well.

Modelling ASF transmission dynamics and control strategies

Transmission model formulation at the pixel scale

We developed a network model to simulate ASF transmission on a pixel-level directed temporal (daily) network of animal movements. Each pixel can be in one of four health states: susceptible (S), exposed (E), infectious (I), and (Q) quarantined. Details of model parameters are described in Table 1 and a graphical description of disease states and their transitions is shown in Figure 2. The model initializes by seeding a single pixel with ASF at a randomly selected daily time point ($t \in T$), run separately for each strain. The pixel, the index case, immediately transitions to the infectious state (I). Transmission is then driven by outgoing animal transfers (between-farm pig movements derived from the SEAPI-RS database (SEAPI-RS, 2018)) from infected pixels to susceptible ones, and assessed at each sequential time point on a daily scale. We assume that ASF is successfully transmitted from infected nodes to susceptible ones at a rate ρ (Table 1). When successful transmission occurs, susceptible nodes transition to exposed immediately, and remain in this state for η_b days, where $\eta_b \in$ PERT(0, $\underline{\eta}$, max(η)) and η is a vector describing the likely incubation period range previously described for two main ASF strains, of high and moderate virulence (Table 1) (Gulenkin et al., 2011; Beltran-Alcrudo et al., 2017). The highly virulent strain mimics the dynamics of the current strain circulation in Europe and Asia, Genotype II (Ge et al., 2018; Mighell and Ward, 2021), while the moderate strain is used to represent a subacute form of the disease. We allow η_b to potentially equal zero (i.e., nodes spend zero days in the exposed state and immediately transition to infected on the following time step) to effectively allow for the possibility that pigs that have already passed their incubation period can be shipped from infected nodes (Howey et al., 2013; Pietschmann et al., 2015). Exposed pixels transition to the infectious state after η_b days, and the simulation continues until the first pixel transitions to the quarantined state. The time pixels spent in the infectious state is variable and depends on within-pixel ASF dynamics (Table 1). Quarantine is triggered when a predefined within-pixel pig mortality is reached. Several mortality trigger scenarios were used to start the deployment of control protocols simulated (Table 1 and Figure 2).

When mortality trigger was set to be zero (i.e., nearly perfect disease detection), named hereafter as "optimistic scenario," we assumed that infectious nodes transition to quarantined as soon as the first animal dies and is identified, which occurs after $\gamma_b$days, where $\gamma_b \in$ PERT(0, $\underline{\gamma}$, max(γ)). The γ parameter is a vector describing the likely time-to-mortality range based on (Beltran-Alcrudo et al., 2017; Guinat et al., 2018), and like $\eta_b$can equal zero to simulate instances when ASF leads to severe clinical infections assumed to be more rapidly detected by passive or active surveillance. When mortality trigger was above zero, we used a within-pixel compartmental Susceptible-Exposed-Infectious-Recovered (SEIR) sub-model describing ASF transmission in local swine populations to estimate the number of days required for mortality trigger percentage of animals within a pixel to die from ASF, and set η_b to this value. The sub-model as given in equations:

$$\frac{dS_{sub}}{dt} = -\beta_{sub} S_{sub} I_{sub},$$
$$\frac{dE_{sub}}{dt} = \beta_{sub} S_{sub} I_{sub} - \left(\frac{1}{\underline{\eta}}\right) E_{sub},$$
$$\frac{dI_{sub}}{dt} = \left(\frac{1}{\underline{\eta}}\right) E_{sub} - \left(\frac{1}{\underline{\gamma}}\right) I_{sub},$$
$$\frac{dR_{sub}}{dt} = \left(\frac{1}{\underline{\gamma}}\right) I_{sub}.$$

Note that the "sub" designation denotes components of the sub-model, and R_{sub} here can be considered to be deceased individuals. We assumed that the number of pigs (*N*) that a pixel contained was equal to the maximum swine-holding capacity of all farms within a pixel, and this sub-model was always initialized with a single infectious pig and *N–1* susceptible pigs. When mortality trigger is above zero, infectious pixels transition after the minimum number of days required for mortality trigger percentage of within-pixel swine populations to be removed from the I_{sub}compartment (i.e., $\min(dt) \mid \frac{R_{sub}}{S_{sub} + E_{sub} + I_{sub} + R_{sub}} \geq$ mortality trigger).When infectious pixels transition to Quarantined, additional pixels may be similarly transitioned, regardless of their current state at time step *t*, in accordance with spatially explicit quarantine protocols (Table 1). For example, control zones of varying sizes (e.g., 1-km, 10-km, or 15-km radii) can be simulated to quarantine all nodes within a fixed distance from the infected node that initially transitioned. All nodes quarantined due to their relationship (e.g., same pig producing company),

pig shipping history, or distance from other nodes were recorded as such in simulation output to support the evaluation of quarantine effects on nearby areas.

We make a number of assumptions in our sub-model. First, we assume that the modeled ASF serotype induces acute symptoms in infected pigs (i.e., our parameterization is not based on per-acute or chronic signs), and infections will always cause death. Second, we assume that local swine populations are static within pixels, regardless of any observed animal transfers. If no information is known about a pixel's swine population or it was reported as zero, the rate at which an infectious pixel transition to Quarantined is determined as if the mortality trigger is equal to zero, regardless of the parameter value of the simulation. Finally, we assume no external transmission sources (e.g., spillover from feral swine populations) contribute to ASF exposure.

The effect of cumulative mortality triggers and control strategies scenarios

Four delayed ASF control triggers based on mortality were simulated individually for each ASF strain (highly and moderately virulent), and later combined with quarantine base control scenarios (Table 1). In the model, ASF infection was detected based on cumulative mortality assumed to be identified by passive surveillance, the cumulative proportion of dead pigs within the simulated thresholds, or in combination with active surveillance from veterinarians or official services investigations on farms with clinical signs or cumulative mortality that trigger an epidemiological investigation, described in Table 1. Model simulations were run across a factorial combination of every variable combination, ASF strains, four mortality triggers, 0%; 1%; 3%; 10%, and the following control measures: 1) established control zones, buffers of a minimum from 0 km to 15 km radius surrounding the affected nodes; 2) implementation of quarantine to all farms of a pig producing company, named hereafter as system-wise, linked to nodes either directly quarantine or infected; 3) backward tracing nodes with direct pig movements to or from nodes under quarantine or infected; and 4) the combination of control zones and the system-wise quarantine. Model simulations factorial combination were the following:

1. High and moderate virulent ASF strains & four mortality triggers (0%; 1%; 3%; 10%) & one quarantine protocol (system-wide).

2. High and moderate virulent ASF strains & four mortality triggers (0%; 1%; 3%; 10%) & 4 buffer distances (0 km; 5 km; 10 km; 15 km) & 2 quarantine protocols (buffer; buffer & system-wide).
3. High and moderate virulent ASF strains & four mortality triggers (0%; 1%; 3%; 10%) & four transfer timeframe levels (1 day; 5 days; 10 days; 15 days) & 1 quarantine protocol (recent pig transfers).

Model outputs and analyses

Each simulation produced three outputs: i) pixel state variables: Susceptible, Exposed, Infectious, and Quarantined, at the final time step; ii) maximum transmission distance and epidemic duration; and iii) the observed transmission and quarantine networks (i.e., who infected or triggered quarantine for whom, and at what time step). As measures of potential severity, we calculated the duration in days, spread capacity in km, and secondary attack rates of ASF epidemics prior to enacted quarantines at the pixel level.

Furthermore, for each quarantine protocol, we report and compare the probability that enacted quarantines resulted in complete ASF containment, (i.e., all infectious and exposed pixels transitioned to the quarantined state), and the mean number of susceptible and "infected" (i.e., exposed of infectious) pixels quarantined. In addition, we derived the total number of quarantined uninfected (i.e., unexposed entities that were quarantined due to their relationship with, or proximity to, a quarantined infected pixel) and infected pixels, as well as the expected number of farms and pigs affected according to each factorial combination. In a series of choropleth maps, we summarize pixel-level probabilities of being infected as a number of secondary cases.

The simulation procedure used each 3-km pixel containing ≥ 1 farm (n = 4,367) as the initially-seeded infectious node 50 times, resulting in 22,708,400 unique simulations. This number of iterations was deemed sufficient to obtain stable outcomes, based on calculations for estimating the appropriate number of simulations in Monte Carlo analyses (Supplementary Material Table S1). In addition, a sensitivity analysis was performed by varying the probability that an animal transfers from an infected node to a susceptible ρ assumed to be 50% and 80% (Table 1 and Supplementary Material). The model was developed in the R (3.6.0 R Core Team,

Vienna, Austria) environment, and simulations were run in RStudio Pro (1.2.5033, RStudio Team, Boston, MA).

Results

The epidemic duration and number of secondary cases were positively correlated with the mortality trigger, while the maximum distance spread was not determined by mortality triggers (Figure 3). The number of days to contain ASF under the optimistic control scenario for the moderately and the highly virulent strain was, on average 11.2 (sd: 2.49) days and 6.50 (sd: 1.59) days, respectively. At 10% mortality the epidemic duration mean was 15.9 (sd: 5.55) days and 13.1 (sd: 7.22) days, respectively (Figure 3; Supplementary Table S2). The average number of secondary cases in simulations was 1.53 (sd: 2.08) and 1.25 (sd: 1.03) pixels at the optimistic scenario, and at 10% mortality 2.75 (sd: 6.71) and 2.56 (sd: 5.95) pixels for the moderated and the highly virulent strain, respectively (Figure 3; Supplementary Table S3). Finally, we also found that the spread distance from initially-infected pixels was similar between both ASF strain variants, on average 23.8 km (sd: 68.4) and 17.9 km (sd: 59.7) in the optimistic scenario and at 10% mortality disease control trigger ASF spread could stretch up to 231.1 km (sd: 78.2) and 29.5 km (sd: 76.0), for the moderately and the highly virulent strain, respectively (Figure 3; Supplementary Table S4).

The predicted spatial distribution pattern of an ASF epidemic is illustrated in Figure 4. An excess number of secondary cases were estimated to occur in densely populated locations in the north and northeast regions of the state. There was no evidence of significant variation in the spatial distribution of ASF strain-specific distribution (Figure 4). However, as expected, early response resulted in fewer successful propagation, especially when the control triggers were activated as soon as the first ASF was found (Figure 4, Supplementary Figure S1 for 3% and 5% mortality trigger maps).

Under the model considered, we predict ASF epidemics will lead to an average of 18.79 (sd: 120) farms and 3,466 (sd: 12,318) pigs for a highly virulent strain and 23.77 (sd: 137) farms and 2,247 (sd: 7,526) pigs for a moderately virulent strain. In comparison, with a mortality based delay of 10% of the population, the epidemic was expected to be nearly double the size, with 42.97 (sd: 119.7) farms and 7,927 (sd: 7,524) pigs for a highly virulent strain and 46.28 (sd: 137) farms and 8,669 (sd: 12,318) pigs for a moderately virulent strain (Table 2).

Mortality-based response triggers and effectiveness of control strategies

Our model also allowed for the investigation of complete disease control (Figure 5; Supplementary Table S5). The less effective strategy across all scenarios was a buffer of less than 15 km. The 15 km buffer outperformed the system-wide quarantine, and ≥ 10 km buffers by themselves outperformed the 1-day shipment trace back. Additionally, when the buffers were used in conjunction with the system-wide control, efficacy increased. The rank-order of control strategies were the same for the both virulent strain and mortality-triggers scenarios (Figure 5) Under the optimistic mortality-base response trigger, the quarantine of pixels that had contact with infected nodes in the previous 15 days was predicted to contain 99.3% of the dispersal of a highly virulent ASF strain and 95.5% for a moderate strain (Figure 5). In contrast, the combination of backward contact tracing with the establishment of control zones of up to 15 km and even adding quarantine of the farms within the same pig producing company showed only marginal improvements if compared with backward contact tracing alone (data not shown). When we simulated 10% of pig mortality, 15-day contact tracing resulted in 88.2% and 87.52% containment probabilities, for the high and the moderate virulence strains, respectively (Figure 5).

The implemented backward contact trace quarantine strategy targeted at infected premises had the lowest total quarantined farms compared with other strategies, regardless of ASF strains and mortality triggers (Figure 6). The overall number of quarantined farms under the 0 km buffer strategy, when compared with 1-day shipment trace back, was similar, the latter control strategy was by far more effective in containing transmission. The number of infected farms quarantined under the 0 km buffer was on average 15.07 farms, similar to one day of recent backward contact trace 16.06 farms (Supplementary Table S6). Whilst the number of susceptible (uninfected) farms quarantined was on average 79.22 farms for the 0 km buffer, while under 1-day shipment trace back exhibited on average 38.10 farms. Overall, the least negative economic and animal welfare impact quarantine strategy was contact tracing-based in which only 0.32% of uninfected farms were predicted to be quarantined, while about 40% of the total uninfected farms would be quarantined via a system-wide control strategy, for example (Supplementary Table S6). For the full details of the simulated quarantine strategies including the success of each intervention in the complete epidemic containment, see Supplementary Table

S6, which also includes results for pixels and the number of pigs predicted to become quarantined.

Discussion

In ASF-free countries, the lack of experience containing large-scale disease emergencies limits the development of evidence-based disease control programs and more precise contingency plans (Halasa et al., 2016b, 2018a; Brown et al., 2020). In this context, we developed a nested multiscale model to simulate the spread of moderately and highly virulent ASF strains in Brazil (Beltran-Alcrudo et al., 2017; Guinat et al., 2018). The model outputs were used to predict the effects of control strategies under mortality-based disease detection plans. We demonstrated that epidemic duration was prolonged and the number of secondary infections was higher under the introduction of a moderately virulent strain. Whilst, the epidemic spread distance was independent of ASF strain type. As expected, ASF propagation was more likely to occur in areas of high pig density (Figure 3). Our model predicted that delaying disease control response under a 10% mortality trigger resulted in an epidemic duration and number of secondary cases that were more than double that of the "optimistic scenario" in which disease control started on the same day that the first dead pig was identified. The most effective simulated intervention strategy, tracing and quarantining previous contacts for the previous 15 days, would avert on average more than 95% of transmissions. Our analysis on the burden caused by the implemented quarantine strategies points again to the advantages of backward contact tracing in which the minimum amount of farms were predicted to be quarantined. In addition, our model showed significantly fewer uninfected (not infected states in the model simulation) nodes were quarantined under this protocol than after implementing any other intervention (Supplementary Table S6).

The simulated epidemic durations were relatively short and directly correlated with the delayed mortality-based control triggers. Our predicted epidemic duration peaked at a maximum of 15 days, similar to other simulated work in which the median epidemic duration was 20 days (min 6-47 days) (Andraud et al., 2019), and with the Denmark work that estimated it to be between 1 to 29 days (Halasa et al., 2016a). The vast majority of the simulations did not result in large outbreaks, the average number of secondary cases varied from 18.79 farms to 46.28 farms depending upon the simulated ASF strain, with limited long-distance spread, which has also been

observed elsewhere (Andraud et al., 2019; Akhmetzhanov et al., 2020). One reason for the similarity could be associated with pig population structure and much less vertically integrated pig farming in the EU and in Brazil when compared with the highly integrated production systems in North America (Galvis, Prada et al., 2021). Another commonality with the simulation done in France was the distances from seed infection to infected nodes estimated to be 300 km (Andraud et al., 2019), while in our study it was restricted to an average distance of 30 km with a maximum spread distance of 603 km (Table S4). In support of our results, China 2018-2019 ASF outbreaks also reported a mean transmission distance to be between 200 km-500 km (Akhmetzhanov et al., 2020). Future studies are needed to explore such epidemic dynamics in more vertical integrated systems such as in the US (Galvis et al., 2020), to better evaluate the role of the effects of changes in herd structure and animal movements on the transmission and control of highly infectious diseases (Halasa, Ward et al., 2020).

We provided the first mapping of ASF epidemic potential in Brazil showing the number of predicted secondary infections, which highlighted areas of a high density of commercial sites with the greatest potential of introduction and spread. Similar spatially explicit disease spread models have been developed to study the spatial distribution of the probability of epidemics for Classical Swine Fever in Great Britain (Porphyre et al., 2017), and also in Bulgaria (Martínez-López et al., 2013), both also concluded that distinct high-risk areas were concentrated in pig-dense regions. While the development of control programs remains a work in progress for affected countries (European Food Safety Authority (EFSA) et al., 2018; Miller and Pepin, 2019), in practice, the maps produced here could be used directly by the local swine industry and by the official veterinary services to guide surveillance activities. An added value of mapping could include, for example, the development of wildlife live passive surveillance of wild boar carcass identification and removal and domestic populations' syndromic surveillance of pig mortality. Whereas the infrastructure and capacity are in place to allow for culling all infected herds and movement bans for neighboring herds have been described as the most effective intervention strategies (Danzetta et al., 2020). The results presented here could be used to build the necessary capabilities and limit the burden on producers with uninfected herds. Our results also provide an opportunity for the implementation of adaptive management, a valuable concept for optimizing the spatial allocation of limited resources.

The results suggested that 15 days backward contact tracing and deployment of quarantine to all movements from nodes in contact with infected or exposed nodes, was the strategy of choice. We could argue that one of the reasons for a better performance of backward contact tracing could be associated with the model mechanics in which explicit local spread is not formally considered. However, previous modeling work in France has concluded that 99% of ASF transmission resulted from between-farm pig movement (Andraud et al., 2019). Even though we have not directly modeled local transmission, our sub-model considers ASF spread dynamics within a pixel's total pig population and implicitly captures unmeasured processes such as shared equipment, tools, and people between neighboring farms within pixels (Halasa et al., 2016a). In addition, our model results reiterate the recommendation of (Halasa et al., 2018a), in which increasing control zones are not expected to significantly shorten ASF epidemics. Finally, we demonstrated multiple control methods when applied in parallel had less than 5% improvement in the control of the ASF propagation.

Pre-emptive depopulation has been described as an ASF control measure in a number of simulation studies and performed during ASF outbreaks, and has proven to be considerably effective in flattening the curve of ASF epidemics (Halasa et al., 2018b; Faverjon et al., 2020). However, pre-emptive depopulation of healthy animals would be met with considerable resistance from the general public and pig producers. Our model predicts that 15-day contact trace would unnecessarily quarantine less than 1% of uninfected farms, while 15 km ring-based quarantine was predicted to massively increase the direct cost by the inflated number of farms needed to undergo quarantine to 8%, see Table S6 for the results of all simulated strategies. Given the real time and electronic movement recorders implemented in the region, contact trace would be the preferred first control strategy in the ASF control program. Even though immediate culling of all pigs at sites where ASF is detected, as well as blanket depopulation within 3-km epidemic zones around infected pig sites (e.g., farms, backyards), used by Chinese authorities, (FAO, 2019c), blanket depopulation based on geospatial proximity is unlikely to stop transmission (Akhmetzhanov et al., 2020).

Limitations and further remarks

We identify a number of limitations in our study associated with simulation rule decisions and data availability. First, our model unit (3-km^2 pixels) targeted spatial locations

where infection would spread and move quickly, thus it was not our objective to make inferences at the farm level. Ultimately, model outputs match the local authorities surveillance system which has been directed towards high and low disease transmission areas. Also, it was not our goal to estimate the contribution of the route of transmission, which could include local transmission, airborne on a smaller scale (de Carvalho Ferreira et al., 2013; Galvis, Jones et al., 2021). However, the next steps could include other routes of transmission including the indirect contact of feed delivery and potential reinfection. Given the importance of wild boars in the spread of ASF, we recognize that there is a need to further develop simulation models to also include the involvement of ASF-outbreaks in wild boar (Hayes et al., 2020).

We simulate ASF spread via pig movements between premises registered with the state veterinary services, which is undoubtedly associated with a large proportion of ASF outbreaks (Andraud et al., 2019; Gao et al., 2020). The potential effects of animal movements from small "backyard" farms on ASF transmission are discounted in our model. It is plausible that the current local surveillance capacity is not sensitive enough to detect small mortality proportions, particularly in small pig farms, future studies considering not only backyard pig movement data but also the sensitivity of disease surveillance should be considered.

Another limitation that must be addressed regards our decision to end simulations as soon as any agent transitions to the quarantined state. In reality, pigs would still continue to be moved throughout the network following the quarantine of one or many areas. Furthermore, we would expect a multi-day response time when quarantining locations, regardless of quarantine protocol (e.g., distance-based quarantine). In our model, however, we do not make any assumptions or predictions regarding how our animal shipment network will behave once nodes are quarantined. Thus, we do not simulate ASF transmission post-quarantine, and we do not allow multi-day response times for triggering quarantine for nodes associated with the initially-quarantined one.

Our model demonstrates which areas are at consistently high risk for pig-infections. The results could be used to predefine risk areas prior to the introduction of ASF but also more broadly other FADs (Gao et al., 2020). In addition, it is pivotal that not only the official veterinary services are aware of the risk distribution of ASF but also that the pig industry receives appropriate information in order to jointly prepare. Given the absence of effective vaccines, the only available measure relies on improving on-farm biosecurity. Thus far there is no clear regulation for the control of ASF-outbreaks in Brazil, but contingency plans against

FADs demand mass depopulation of infected farms and the investigation of all herds within the surveillance zones. Even though recent outbreaks in Europe, Estonia, showed that for large pig farms mortality is not the best option for early detections of an ASF outbreak (Nurmoja et al., 2020). Future studies are needed, for example considering the mortality levels at barn and pen-level (Faverjon et al., 2020). It is worth noting that even though fatality rates under field conditions have been high, while initial mortality, depending on the ASF strain, have been reported to be low in especially in large commercial sites (C. et al., 2018; Lamberga et al., 2020; Nurmoja et al., 2020), under such scenarios it could be mistaken for other endemic diseases such as porcine reproductive and respiratory syndrome (Faverjon et al., 2020).

Conclusion

The vast majority of simulations predicted short epidemic durations and resulted in relatively small outbreaks. Early mortality-based ASF detection significantly curbed the epidemic size, especially when a best-case scenario, in which quarantine is applied as the first infected pig dies, is compared with 10% pig mortality as a quarantine trigger. Our modeling analyses have given insight into transmission dynamics and ASF spatial distribution in which it may persist, thus the probability map of secondary cases could be used to define priority and represent the first steps for well-programmed surveillance. Although our model only considered quarantine as control strategies, the best intervention regardless of delayed disease control triggers was backward contact tracing for 15 days. Additional quarantine efforts based either on ring-based strategies or pig production level did not significantly improve control efficacy. Moreover, the best control strategy was independent of viral strain virulence through all simulated scenarios. Finally, the results of this study can be used to make informed decisions at the state of Rio Grande do Sul Brazil to implement target ASF surveillance activities and used in preparation for future outbreaks. Our mapping results showed areas in which ASF spread is more likely, therefore further preparation would be beneficial in such areas.

Acknowledgments

The primary funding support of this project is from Global Health, College of Veterinary Medicine at North Carolina State University and by the Fundo de Desenvolvimento e Defesa Sanitária Animal (FUNDESA-RS).

Authors' contributions

TF, CZ, and GM conceived the study. GM designed the study and coordinated data collection with the assistant of FPNL. TF and GM conducted data processing, cleaning, designed the model, and simulated scenarios with the assistance of CZ. TF, CZ, and GM designed the computational analysis. TF and GM wrote and edited the manuscript. All authors discussed the results and critically reviewed the manuscript. CZ and GM secured the funding.

Conflict of interest

All authors confirm that there are no conflicts of interest to declare.

Ethical statement

The authors confirm the ethical policies of the journal, as noted on the journal's author guidelines page. Since this work did not involve animal sampling nor questionnaire data collection by the researchers there was no need for ethics permits.

Data Availability Statement

The data that support the findings of this study are not publicly available and are protected by confidential agreements, therefore, are not available.

References

Akhmetzhanov, A.R., S. Jung, H. Lee, N. Linton, Y. Yang, B. Yuan, and H. Nishiura, 2020: Reconstruction and analysis of the transmission network of African swine fever in People's Republic of China, August 2018–September 2019. *2021*DOI: 10.1101/2020.07.12.199760.

Andraud, M., T. Halasa, A. Boklund, and N. Rose, 2019: Threat to the French Swine Industry of African Swine Fever: Surveillance, Spread, and Control Perspectives. *Front. Vet. Sci.* **6**, 248, DOI: 10.3389/fvets.2019.00248.

Bellini, S., D. Rutili, and V. Guberti, 2016: Preventive measures aimed at minimizing the risk of African swine fever virus spread in pig farming systems. *Acta Vet Scand* **58**, 82, DOI: 10.1186/s13028-016-0264-x.

Beltran-Alcrudo, D., M. Arias, C. Gallardo, S.A. Kramer, and M.-L. Penrith, 2017: African swine fever (ASF) detection and diagnosis-A manual for veterinarians. *FAO Animal Production and Health Manual* **19**, 88.

Bradhurst, R.A., S.E. Roche, I.J. East, P. Kwan, and M.G. Garner, 2015: A hybrid modeling

approach to simulating foot-and-mouth disease outbreaks in Australian livestock. *Front. Environ. Sci.* **3**, DOI: 10.3389/fenvs.2015.00017.

Brown, V.R., R.S. Miller, S.C. McKee, K.H. Ernst, N.M. Didero, R.M. Maison, M.J. Grady, and S.A. Shwiff, 2020: Risks of introduction and economic consequences associated with African swine fever, classical swine fever and foot-and-mouth disease: A review of the literature. *Transbound Emerg Dis*tbed.13919, DOI: 10.1111/tbed.13919.

C., G., N. I., S. A., D. V., S. A., M. E., P. C., N. R., and A. M., 2018: Evolution in Europe of African swine fever genotype II viruses from highly to moderately virulent. *Veterinary Microbiology* **219**, 70–79, DOI: 10.1016/j.vetmic.2018.04.001.

Chenais, E., K. Depner, V. Guberti, K. Dietze, A. Viltrop, and K. Ståhl, 2019: Epidemiological considerations on African swine fever in Europe 2014–2018. *Porc Health Manag* **5**, 6, DOI: 10.1186/s40813-018-0109-2.

Costard, S., B. Wieland, W. de Glanville, F. Jori, R. Rowlands, W. Vosloo, F. Roger, D.U. Pfeiffer, and L.K. Dixon, 2009: African swine fever: how can global spread be prevented? *Phil. Trans. R. Soc. B* **364**, 2683–2696, DOI: 10.1098/rstb.2009.0098.

Danzetta, M.L., M.L. Marenzoni, S. Iannetti, P. Tizzani, P. Calistri, and F. Feliziani, 2020: African Swine Fever: Lessons to Learn From Past Eradication Experiences. A Systematic Review. *Front. Vet. Sci.* **7**, 296, DOI: 10.3389/fvets.2020.00296.

de Carvalho Ferreira, H.C., E. Weesendorp, S. Quak, J.A. Stegeman, and W.L.A. Loeffen, 2013: Quantification of airborne African swine fever virus after experimental infection. *Veterinary Microbiology* **165**, 243–251, DOI: 10.1016/j.vetmic.2013.03.007.

Dellicour, S., D. Desmecht, J. Paternostre, C. Malengreaux, A. Licoppe, M. Gilbert, and A. Linden, 2020: Unravelling the dispersal dynamics and ecological drivers of the African swine fever outbreak in Belgium. (Andrew Park, Ed.)*J Appl Ecol* **57**, 1619–1629, DOI: 10.1111/1365-2664.13649.

Díaz-Emparanza, I., 2002: Is a small Monte Carlo analysis a good analysis?: Checking the size, power and consistency of a simulation-based test. *Statistical Papers* **43**, 567–577, DOI: 10.1007/s00362-002-0124-9.

Dixon, L.K., K. Stahl, F. Jori, L. Vial, and D.U. Pfeiffer, 2020: African Swine Fever Epidemiology and Control. *Annu. Rev. Anim. Biosci.* **8**, 221–246, DOI: 10.1146/annurev-animal-021419-083741.

European Commission, 2020 (29. April): Strategic approach to the management of African Swine Fever for the EU – Rev. February 2020. . DIRECTORATE-GENERAL FOR HEALTH AND FOOD SAFETY.

European Food Safety Authority (EFSA), A. Boklund, B. Cay, K. Depner, Z. Földi, V. Guberti, M. Masiulis, A. Miteva, S. More, E. Olsevskis, P. Šatrán, M. Spiridon, K. Stahl, H. Thulke, A. Viltrop, G. Wozniakowski, A. Broglia, J. Cortinas Abrahantes, S. Dhollander, A. Gogin, F. Verdonck, L. Amato, A. Papanikolaou, and C. Gortázar, 2018: Epidemiological analyses of African swine fever in the European Union (November 2017 until November 2018). *EFS2* **16**, DOI: 10.2903/j.efsa.2018.5494.

Ezanno, P., M. Andraud, G. Beaunée, T. Hoch, S. Krebs, A. Rault, S. Touzeau, E. Vergu, and S. Widgren, 2020: How mechanistic modelling supports decision making for the control of enzootic infectious diseases. *Epidemics* **32**, 100398, DOI: 10.1016/j.epidem.2020.100398.

Faverjon, C., A. Meyer, K. Howden, K. Long, L. Peters, and A. Cameron, 2020: Risk-based early detection system of African Swine Fever using mortality thresholds. *Transbound Emerg Dis*tbed.13765, DOI: 10.1111/tbed.13765.

Ferdousi, T., S.A. Moon, A. Self, and C. Scoglio, 2019: Generation of swine movement network and analysis of efficient mitigation strategies for African swine fever virus. (Willem F. de Boer, Ed.)*PLoS ONE* **14**, e0225785, DOI: 10.1371/journal.pone.0225785.

Gallardo, M.C., A. de la T. Reoyo, J. Fernández-Pinero, I. Iglesias, M.J. Muñoz, and M.L. Arias, 2015: African swine fever: a global view of the current challenge. *Porc Health Manag* **1**, 21, DOI: 10.1186/s40813-015-0013-y.

Galvis, J.A., C.M. Jones, J.M. Prada, C.A. Corzo, and G. Machado, 2021: The between-farm transmission dynamics of Porcine Epidemic Diarrhea Virus: A short-term forecast modeling comparison and the effectiveness of control strategies. *Transbound Emerg Dis*tbed.13997, DOI: 10.1111/tbed.13997.

Galvis, J.A., J.M. Prada, C.A. Corzo, and G. Machado, 2020: Modeling the transmission and vaccination strategy for porcine reproductive and respiratory syndrome virus (preprint). Ecology.

Galvis, J.A., J.M. Prada, C.A. Corzo, and G. Machado, 2021: Modeling the transmission and vaccination strategy for porcine reproductive and respiratory syndrome virus. *Transboundary and Emerging Diseases*tbed.14007, DOI: 10.1111/tbed.14007.

Gao, L., X. Sun, H. Yang, Q. Xu, J. Li, J. Kang, P. Liu, Y. Zhang, Y. Wang, and B. Huang, 2020: Epidemic situation and control measures of African Swine Fever Outbreaks in China 2018-2020. *Transboundary and Emerging Diseases*tbed.13968, DOI: 10.1111/tbed.13968.

Ge, S., J. Li, X. Fan, F. Liu, L. Li, Q. Wang, W. Ren, J. Bao, C. Liu, H. Wang, Y. Liu, Y. Zhang, T. Xu, X. Wu, and Z. Wang, 2018: Molecular Characterization of African Swine Fever Virus, China, 2018. *Emerg. Infect. Dis.* **24**, 2131–2133, DOI: 10.3201/eid2411.181274.

Guinat, C., T. Porphyre, A. Gogin, L. Dixon, D.U. Pfeiffer, and S. Gubbins, 2018: Inferring within-herd transmission parameters for African swine fever virus using mortality data from outbreaks in the Russian Federation. *Transbound Emerg Dis* **65**, e264–e271, DOI: 10.1111/tbed.12748.

Guinat, C., T. Vergne, C. Jurado-Diaz, J.M. Sánchez-Vizcaíno, L. Dixon, and D.U. Pfeiffer, 2017: Effectiveness and practicality of control strategies for African swine fever: what do we really know? *Veterinary Record* **180**, 97–97, DOI: 10.1136/vr.103992.

Gulenkin, V.M., F.I. Korennoy, A.K. Karaulov, and S.A. Dudnikov, 2011: Cartographical analysis of African swine fever outbreaks in the territory of the Russian Federation and computer modeling of the basic reproduction ratio. *Preventive Veterinary Medicine* **102**, 167–174, DOI: 10.1016/j.prevetmed.2011.07.004.

Halasa, T., A. Bøtner, S. Mortensen, H. Christensen, N. Toft, and A. Boklund, 2016a: Simulating the epidemiological and economic effects of an African swine fever epidemic in industrialized swine populations. *Veterinary Microbiology* **193**, 7–16, DOI: 10.1016/j.vetmic.2016.08.004.

Halasa, T., A. Bøtner, S. Mortensen, H. Christensen, N. Toft, and A. Boklund, 2016b: Control of African swine fever epidemics in industrialized swine populations. *Veterinary Microbiology* **197**, 142–150, DOI: 10.1016/j.vetmic.2016.11.023.

Halasa, T., A. Bøtner, S. Mortensen, H. Christensen, S.B. Wulff, and A. Boklund, 2018a: Modeling the Effects of Duration and Size of the Control Zones on the Consequences of a Hypothetical African Swine Fever Epidemic in Denmark. *Front. Vet. Sci.* **5**, 49, DOI: 10.3389/fvets.2018.00049.

Halasa, T., A. Bøtner, S. Mortensen, H. Christensen, S.B. Wulff, and A. Boklund, 2018b: Modeling the Effects of Duration and Size of the Control Zones on the Consequences of a Hypothetical African Swine Fever Epidemic in Denmark. *Front. Vet. Sci.* **5**, 49, DOI: 10.3389/fvets.2018.00049.

Halasa, T., K. Græsbøll, M. Denwood, L.E. Christensen, and C. Kirkeby, 2020: Prediction Models in Veterinary and Human Epidemiology: Our Experience With Modeling Sars-CoV-2 Spread. *Front. Vet. Sci.* **7**, 513, DOI: 10.3389/fvets.2020.00513.

Halasa, T., M.P. Ward, and A. Boklund, 2020: The impact of changing farm structure on foot-and-mouth disease spread and control: A simulation study. *Transbound Emerg Dis* **67**, 1633–1644, DOI: 10.1111/tbed.13500.

Hayes, B.H., M. Andraud, L.G. Salazar, N. Rose, and T. Vergne, 2020: Mechanistic modeling of African swine fever: A systematic review. *arXiv:2011.10126 [q-bio]*.

Heesterbeek, H., R.M. Anderson, V. Andreasen, S. Bansal, D. De Angelis, C. Dye, K.T.D. Eames, W.J. Edmunds, S.D.W. Frost, S. Funk, T.D. Hollingsworth, T. House, V. Isham, P. Klepac, J. Lessler, J.O. Lloyd-Smith, C.J.E. Metcalf, D. Mollison, L. Pellis, J.R.C. Pulliam, M.G. Roberts, C. Viboud, and Isaac Newton Institute IDD Collaboration, 2015: Modeling infectious disease dynamics in the complex landscape of global health. *Science* **347**, aaa4339–aaa4339, DOI: 10.1126/science.aaa4339.

Howey, E.B., V. O'Donnell, H.C. de Carvalho Ferreira, M.V. Borca, and J. Arzt, 2013: Pathogenesis of highly virulent African swine fever virus in domestic pigs exposed via intraoropharyngeal, intranasopharyngeal, and intramuscular inoculation, and by direct contact with infected pigs. *Virus Research* **178**, 328–339, DOI: 10.1016/j.virusres.2013.09.024.

Lamberga, K., E. Oļševskis, M. Seržants, A. Bērziņš, A. Viltrop, and K. Depner, 2020: African Swine Fever in Two Large Commercial Pig Farms in LATVIA—Estimation of the High Risk Period and Virus Spread within the Farm. *Veterinary Sciences* **7**, 105, DOI: 10.3390/vetsci7030105.

Machado, G., J.A. Galvis, F.P.N. Lopes, J. Voges, A.A.R. Medeiros, and N.C. Cárdenas, 2020: Quantifying the dynamics of pig movements improves targeted disease surveillance and control plans. *Transbound. Emerg. Dis*tbed.13841, DOI: 10.1111/tbed.13841.

Martínez-López, B., B. Ivorra, A.M. Ramos, E. Fernández-Carrión, T. Alexandrov, and J.M. Sánchez-Vizcaíno, 2013: Evaluation of the risk of classical swine fever (CSF) spread from backyard pigs to other domestic pigs by using the spatial stochastic disease spread model Be-FAST: The example of Bulgaria. *Veterinary Microbiology* **165**, 79–85, DOI: 10.1016/j.vetmic.2013.01.045.

Mighell, E., and M. Ward, 2021: African Swine Fever spread across Asia, 2018−2019. *Transbound Emerg Dis*tbed.14039, DOI: 10.1111/tbed.14039.

Miller, R.S., and K.M. Pepin, 2019: BOARD INVITED REVIEW: Prospects for improving management of animal disease introductions using disease-dynamic models. *Journal of Animal Science* **97**, 2291–2307, DOI: 10.1093/jas/skz125.

Nielsen, J.P., T.S. Larsen, T. Halasa, and L.E. Christiansen, 2017: Estimation of the transmission dynamics of African swine fever virus within a swine house. *Epidemiol. Infect.* **145**, 2787–2796, DOI: 10.1017/S0950268817001613.

Nurmoja, I., K. Mõtus, M. Kristian, T. Niine, K. Schulz, K. Depner, and A. Viltrop, 2020: Epidemiological analysis of the 2015–2017 African swine fever outbreaks in Estonia. *Preventive Veterinary Medicine* **181**, 104556, DOI: 10.1016/j.prevetmed.2018.10.001.

Pietschmann, J., C. Guinat, M. Beer, V. Pronin, K. Tauscher, A. Petrov, G. Keil, and S. Blome, 2015: Course and transmission characteristics of oral low-dose infection of domestic pigs and European wild boar with a Caucasian African swine fever virus isolate. *Arch Virol* **160**, 1657–1667, DOI: 10.1007/s00705-015-2430-2.

Porphyre, T., C. Correia-Gomes, M.E. Chase-Topping, K. Gamado, H.K. Auty, I. Hutchinson, A. Reeves, G.J. Gunn, and M.E.J. Woolhouse, 2017: Vulnerability of the British swine industry to classical swine fever. *Sci Rep* **7**, 42992, DOI: 10.1038/srep42992.

Salguero, F.J., 2020: Comparative Pathology and Pathogenesis of African Swine Fever Infection in Swine. *Front. Vet. Sci.* **7**, 282, DOI: 10.3389/fvets.2020.00282.

Sánchez-Cordón, P.J., M. Montoya, A.L. Reis, and L.K. Dixon, 2018: African swine fever: A re-emerging viral disease threatening the global pig industry. *The Veterinary Journal* **233**, 41–48, DOI: 10.1016/j.tvjl.2017.12.025.

Sauter-Louis, C., J.H. Forth, C. Probst, C. Staubach, A. Hlinak, A. Rudovsky, D. Holland, P. Schlieben, M. Göldner, J. Schatz, S. Bock, M. Fischer, K. Schulz, T. Homeier-Bachmann, R. Plagemann, U. Klaaß, R. Marquart, T.C. Mettenleiter, M. Beer, F.J. Conraths, and S. Blome, 2020: Joining the club: First detection of African swine fever in wild boar in Germany. *Transbound Emerg Dis*tbed.13890, DOI: 10.1111/tbed.13890.

SEAPI-RS, 2018: Secretaria da Agricultura, Pecuária e arrigação. *SEAPI*.

USDA-APHIS, 2020: FAD PReP. *USDA-Animal Health*.

Vose, D., 2008: Risk Anaysis - A Quantitative Guide.*John Wiley & Sons*.

Winston, W.L., 2020: Simulation Modeling Using @Risk. Brooks/Cole.

Table List

Table 1. Overview of variables and key model parameters. All units are days unless otherwise noted

Parameters/ Variables	**Description**	**Model values**
T	Vector of sequential timesteps.	1:1,440 days
ρ	The probability that an animal transfers from an infected node to a susceptible one will cause the latter to transition to the exposed state.	50%* 80%* 100%
η	Vector of likely incubation-period length for acute ASF serotypes (Gulenkin et al., 2011; Beltran-Alcrudo et al., 2017).	4:7 days
η_b	Length of ASF incubation period (days), drawn from the beta-PERT distribution (Vose, 2008) parameterized withη values.	$\eta_b \in$ PERT(0, $\underline{\eta}$, max(η))

γ	Vector of likely time-to-mortality for acute ASF serotypes (Beltran-Alcrudo et al., 2017; Guinat et al., 2018). Varies with high and moderate virulence.	γ_{high} = 6:9 γ_{mod} = 11:15
γ_b	Time-to-mortality (days), drawn from the beta-PERT distribution (Vose, 2008) parameterized with γ values. This is only relevant when the simulation mortality trigger is > 0%.	$\gamma_b \in$ PERT(0, $\underline{\gamma}$, max(γ))
β_{sub}	Daily within-pixel ASF transmission coefficient. This is the weighted median of estimated betas presented by (Guinat et al., 2018; Hayes et al., 2020), and first used by (Ferdousi et al., 2019) in their ASF transmission model.	1.679
Virulence	Variable modulating time-to-mortality values.	High, Moderate
Mortality trigger	The proportion of the within-pixel population mortality required to trigger quarantine and intervention scenarios.	0% 1% 3% 10%
Control strategies	**Description**	**Model values**
Quarantine protocol	Procedures for subsequently quarantining pixels nearby or related to those that initially transition from the infectious state. **1) Buffer:** quarantine pixels within a pre-specified distance (ring) to the first quarantined node (control zone) **2) Pig production system-wide:** quarantine pixels sharing a production system with the first quarantined. **3) Buffer & system-wide:** a combination of buffer and system-wide procedures. **4) Recent pig transfers:** quarantine pixels with any edges connected to the first quarantined node within a pre-specified time period.	1) buffer 2) system-wide 3) buffer & system-wide 4) recent transfers
Buffer distance	Distance from initially-quarantined pixels within which other pixels will be additionally quarantined.	0 km 5 km 10 km 15 km
Transfer time frame	Number of time steps (days) within which any observed edges between non-quarantined pixels and initially-quarantined ones will trigger quarantine transition.	1 day 5 days 10 days 15 days

*These □ values were only used to parameterize simulations intended for sensitivity analyses reported in Supplemental Material and were excluded from all simulations described in the main text.

Table 2. Predicted quarantine consequences of two ASF strain outbreaks under different mortality triggers. The average and standard deviation in brackets of the predicted quarantined pixels, farms, and animals are shown.

ASF strain virulence	**0% Mortality trigger**			**1% Mortality trigger**			**3% Mortality trigger**			**10% Mortality trigger**		
	Pixels	*Farm*	*Pigs*	*Pixels*	*Farm*	*Pigs*	*Pixels*	*Farm*	*Pigs*	*Pixels*	*Farm*	*Pigs*
Moderate	1.53 (2.08)	23.77 (136.75)	3,466 (12,318)	2.01 (4.1)	32.62 (170.48)	5,573.18 (21,745.37)	2.3 (5.13)	37.9 (189.47)	6,789.7 (26,226.59)	2.75 (2.08)	46.28 (136.74)	8,668.59 (12,317.84)
High	1.25 (1.03)	18.79 (119.7)	2,247 (7,525.49)	1.92 (3.77)	31.06 (164.62)	5,220.48 (20,408.94)	2.19 (4.69)	35.9 (181.94)	6,352.81 (24,453.79)	2.56 (1.03)	42.97 (119.7)	7,926.92 (7,525.49)

Figure Legend

Figure 1. Study area. The study area, Rio Grande do Sul Brazil, was gridded into 3 km x 3 km cells (pixels) to represent the total number of pigs per pixel.

Figure 2. Schematic of state transitions for between pixels model. Solid lines indicate fixed transitions that are bound to occur, dashed lines represent potential transitions that may occur upon quarantine protocols. Individuals in the Susceptible state ($s \in$ S) will transition to the Exposed state with a probability of ρ if an edge exists between Susceptible individual s and Infectious individual i ($i \in$ I) during a defined time period in our dynamic contact network. Individuals in the Exposed state transition to the Infectious state at a fixed rate, and individuals in the Infectious state transition to Quarantined at a fixed rate, as well. Individuals in any state can transition to Quarantined in accordance with pre-determined quarantine protocol if they share a specific relationship with the first node to transition from I to Q (i.e., q′).

Figure 3. ASF epidemic outcomes for a highly or moderately virulent strain. The predicted number of days in an ASF epidemic using different mortality levels to trigger control interventions (top). The predicted number of secondarily infected pixels (middle). The maximum distance from initial seeded infection to all secondary infections during the course of the simulations (bottom).

Figure 4. Average infected pixels (3 km by 3 km). Pixels highlighted correspond to simulated average secondary cases under the simulated optimistic scenario (quarantine is triggered as the first ASF case is identified), left panel, compared with a delayed response trigger after a cumulative 10% of the pig mortality, right panel.

Figure 5. The predicted number of ASF transmission events successfully controlled by mortality-trigger and virulence combinations. The "no transmission" line indicates the percent of simulations in which no secondary transmission occurred, and thus, quarantining only the initially-seeded node was sufficient to completely contain the outbreak.

Figure 6. The predicted number of quarantined farms per mortality-trigger, ASF strain, control strategies, and infected and uninfected farms. Summary of simulated outputs the total number of quarantined farms, regardless of its infection state. Table S6 included the breakdown of infected and uninfected states of the quarantined pixels, farms, and number of pigs.

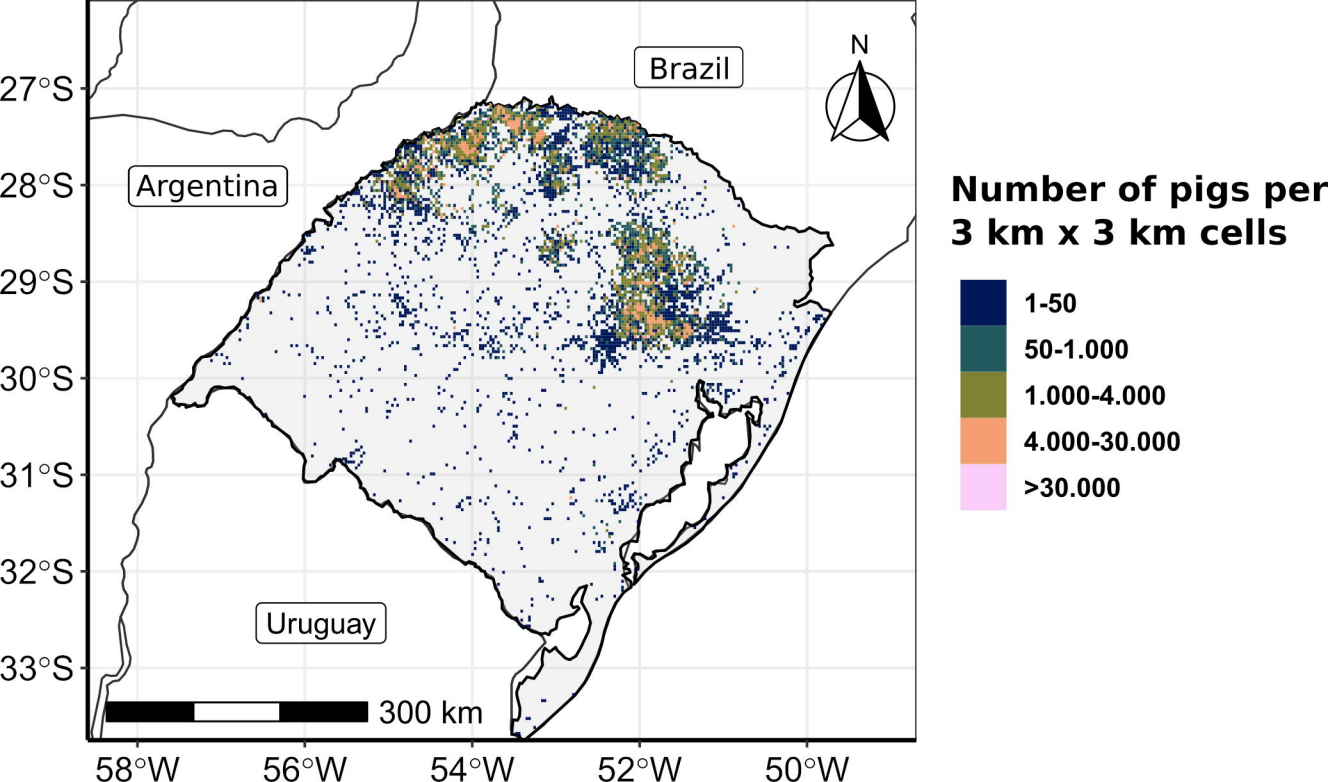
Brazil
Argentina
Uruguay
N
27°S
28°S
29°S
30°S
31°S
32°S
33°S
58°W
56°W
54°W
52°W
50°W
300 km
Number of pigs per
3 km x 3 km cells
1-50
50-1.000
1.000-4.000
4.000-30.000
>30.000

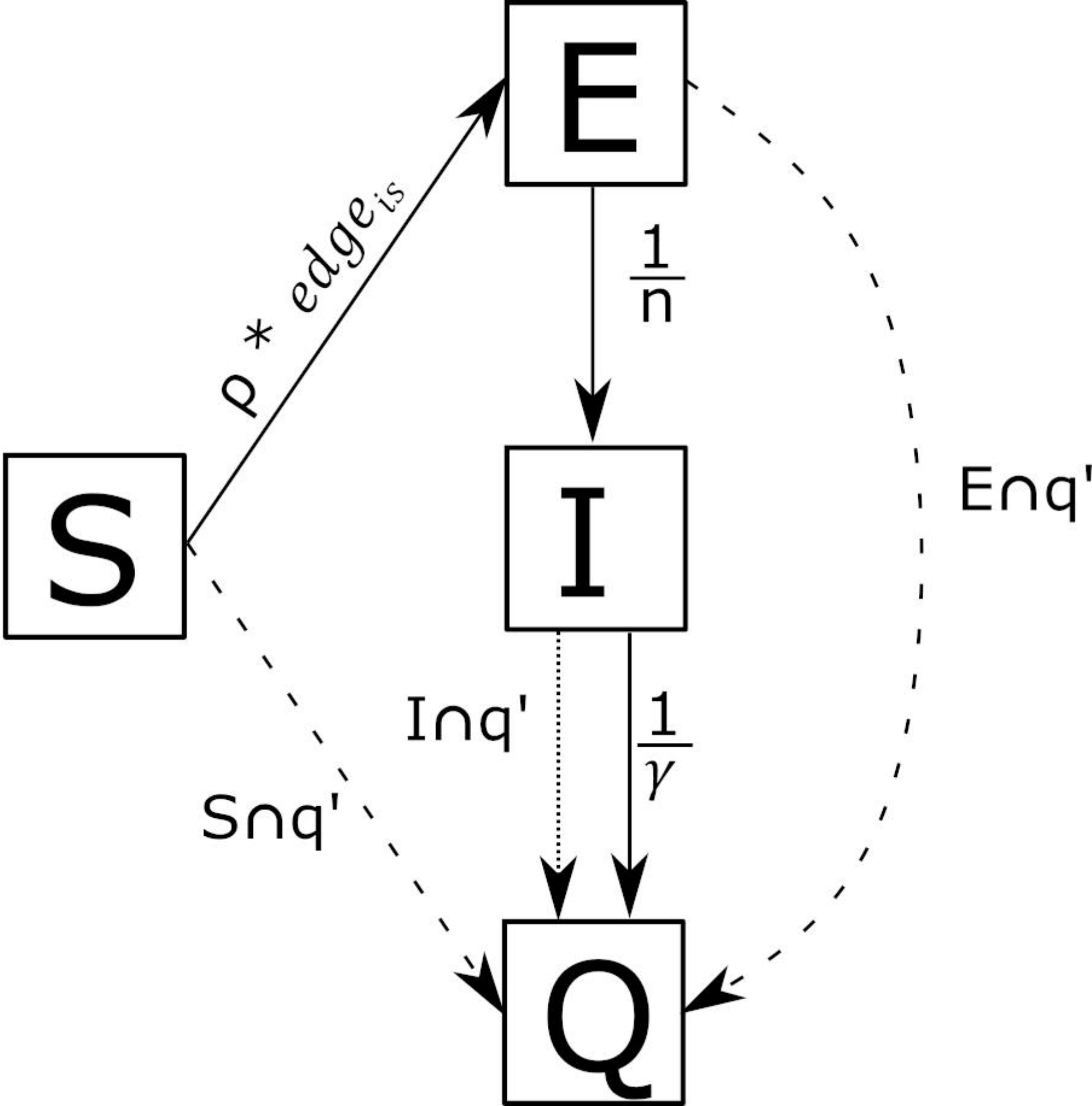
E
S
I
Q
$\rho * edge_{is}$
$\frac{1}{n}$
$\frac{1}{\gamma}$
Enq'
Inq'
Snq'

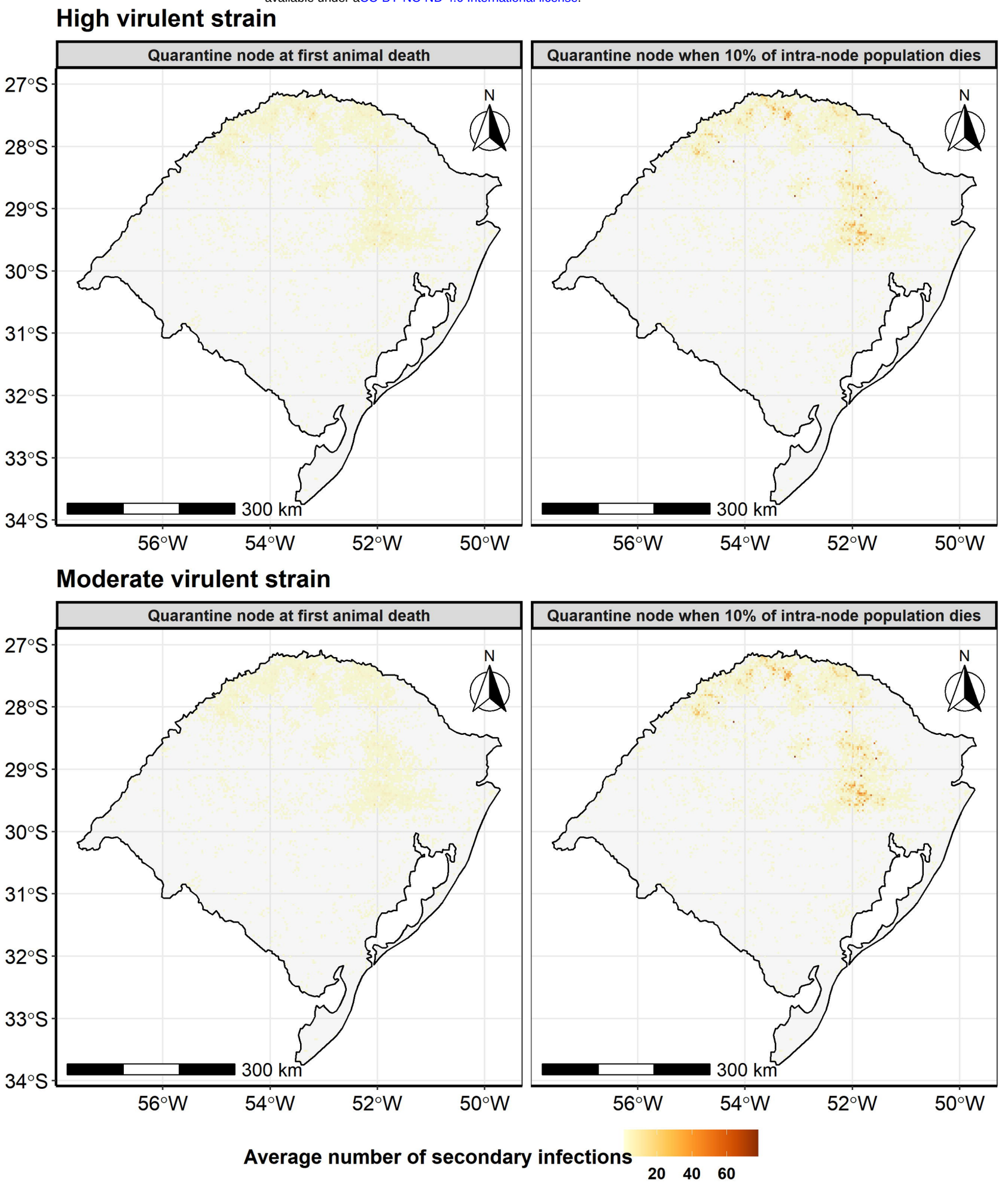

moderate

high

0% mortality

1% mortality

3% mortality

10% mortality

Percent of simulations (%)

100%

95%

90%

85%

80%

00 km
05 km
10 km
15 km
system-wide
00 km
05 km
10 km
15 km
01 days
05 days
10 days
15 days

Quarantine protocol

buffer
buffer & system-wide
recent transfers
system-wide

no transmission